Nonlinear Pile-Head Macro-Element Model: SSI effects on the Seismic Response of a Monoshaft-Supported Bridge

A.A. Correia
ROSE School, IUSS Pavia, Italy

A. Pecker
Geodynamique et Structure, Bagneux, France

S.L. Kramer
University of Washington, Seattle, USA

R. Pinho
University of Pavia, Italy

SUMMARY:
An innovative pile-head macro-element model, recently proposed for the simulation of inertial soil-structure interaction effects in the seismic analysis of structures supported on long piles, is briefly presented. After its validation through comparison with both numerical and experimental results, such approach is used for analysing the seismic response of a monoshaft-supported bridge by means of incremental dynamic analyses. Different support conditions are examined, exposing the relevance of soil-structure interaction effects for such structure, and a large set of ground motions are considered. The additional deformability of the soil-foundation system, when compared to the fixed-base case, is of paramount importance for both maximum and residual deformations of the bridge, which are highly dependent on the significance of second-order effects. Considering the balance between simulation accuracy, numerical stability and computational effort, the proposed macro-element is demonstrated to be a cost-effective tool for performance-based seismic design.

Keywords: macro-element; pile-head; soil-structure interaction; nonlinear response; bridge design

1. INTRODUCTION

The pile-head macro-element model recently proposed by Correia (2011) represents an extension of the macro-element concept, previously developed for structures on shallow foundations with significant success (e.g. Figini et al., 2011), to the case of deep foundations. Despite the assumed simplifications, it captures all relevant features of the entire soil-structure system's response to inertial pile-head loading. Fig. 1 illustrates the characteristic soil response for a laterally loaded long pile, namely: a soil passive wedge failure at shallow depths and flow-around failure at larger depths, with a possible gap formation on the back of the pile.

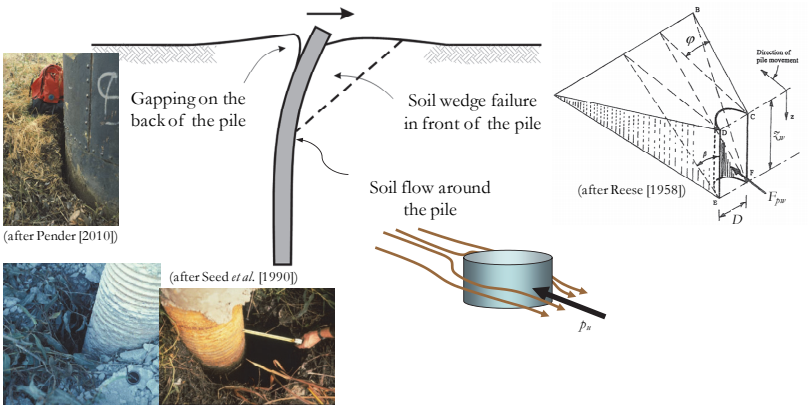

Figure 1. Characteristic soil response for pile-head lateral loading

Accurate estimates of maximum and residual seismic displacements, essential within the framework of performance-based design (PBD), may now also be obtained in a cost-effective manner when deep foundations are involved. This work briefly presents the proposed pile-head macro-element approach and its validation. Afterwards, it is used for analysing the seismic response of a monoshaft-supported bridge through incremental dynamic analyses (IDAs).

2. PILE-HEAD MACRO-ELEMENT FORMULATION AND VALIDATION

Alternative models for analysing soil-structure interaction (SSI) effects on structures with piled foundations, either by using the concept of experimentally determined *p-y* curves or by using a pile-head condensation of the response as adopted herein, are depicted in Fig. 2a. On the other hand, the soil is assumed to be saturated and, during seismic action, impervious and not susceptible to liquefaction. It thus presents an undrained seismic response, for which the Tresca failure criterion is assumed to be valid. Fig. 2b represents the two simplified geotechnical scenarios considered in this work in terms of undrained shear strength (S_u) distribution along the depth of the soil deposit: constant or linear.

The proposed pile-head macro-element model represents the nonlinear lateral behaviour of a single, vertical, pile/column and its surrounding soil, with the following basic components:

i) initial elastic impedances, representing the small-strain behaviour of the system;
ii) gapping behaviour and gap evolution model;
iii) failure mechanism and corresponding ultimate loading surface, representing the large-strain behaviour of the pile and soil;
iv) bounding surface plasticity model for the pile-head resultant generalised forces and corresponding displacements, which makes the transition between the small-strain and large-strain response domains.

Each of these components is briefly described in the following.

2.1. Failure Surface

In this work, the failure surface and mechanism for laterally loaded piles were determined through the kinematic approach of yield design theory, which is somewhat similar to a limit analysis approach (Salençon, 1983). A completely compatible and continuous virtual velocity field was proposed based on a three-dimensional incompressible soil flow with a possible tangent or detaching discontinuity at the pile face only (Correia, 2011). The geometry of such mechanism is according to Fig. 1: it includes conical active and passive soil wedges having different dimensions and velocity fields, with a possible gap formation on the back of the pile, and a continuous transition to a flow-around movement with depth, which becomes a planar flow-around solution below the soil wedge depth. The pile velocity field at failure includes a plastic hinge forming at a depth z_h, with almost rigid behaviour of the remaining pile length.

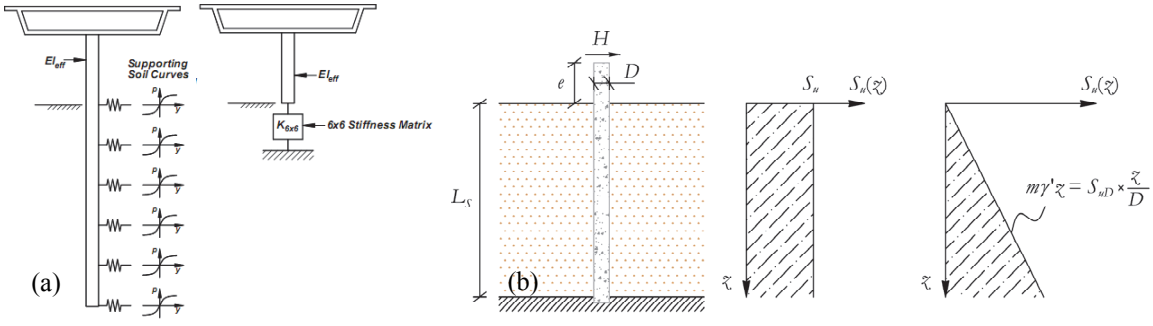

Figure 2. (a) Alternative analysis models (Hutchinson et al., 2002) for laterally loaded monoshaft supports in bridges; (b) simplified geotechnical scenarios considered

The minimum upper-bound failure mechanism parameters and the corresponding failure surface were determined through a nonlinear constrained optimisation procedure, making use of the existing tools in the software MATLAB (MathWorks, 2009). Such procedure was applied in a parametric study considering most common soil-pile characteristics (Correia, 2011). Subsequently, for a straightforward numerical implementation of the plasticity formulation, it was proposed that the pile-head failure surface was approximated by a rounded curve, which corresponds to a distorted superellipse. It is shown in Fig. 3 for a particular case, while the comparison of such curve with all the optimisation results of the parametric study for both soil profiles is also depicted in the same figure.

2.2. Initial Elastic Response and Gapping Model

The initial elastic response of the pile-head macro-element was assumed to be characterised by approximate expressions for pile-head equivalent-linear impedances, such as the ones proposed by Gazetas (1991) and adopted in EC8 – Part 5 (2003). These represent both the dynamic stiffnesses of the macro-element as well as the dynamic radiation damping behaviour.

Regarding the gapping model, Fig. 1 showed evidence of gapping behaviour observed during seismic events. Fig. 4, on the other hand, represents the results obtained from OpenSees (McKenna et al., 2000) using an advanced three-dimensional finite element model that considers both elastic and nonlinear soil behaviour, for the constant S_u soil profile. The gapping influence on the corresponding numerical response to pile-head loading, shown therein, is clear.

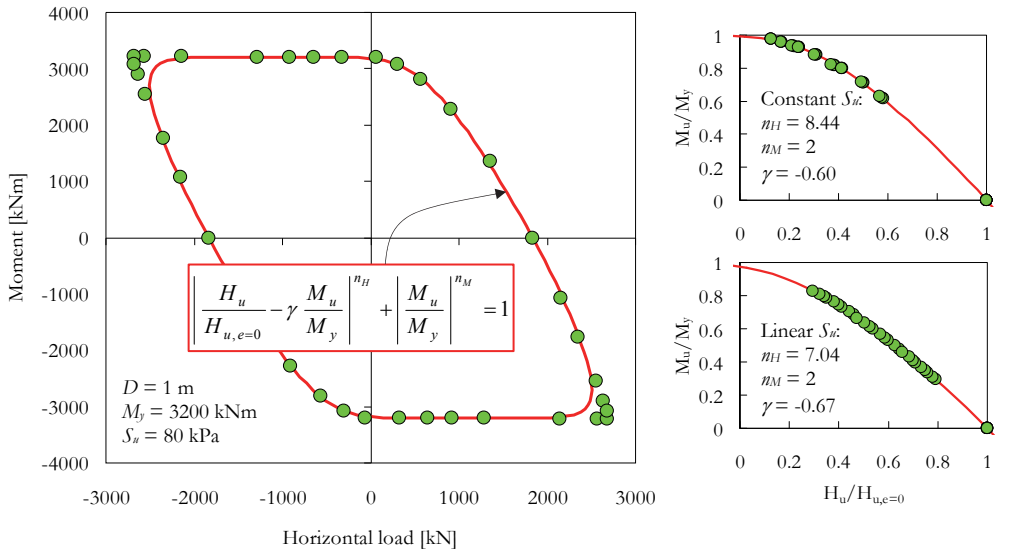

Figure 3. Failure surface and superellipse

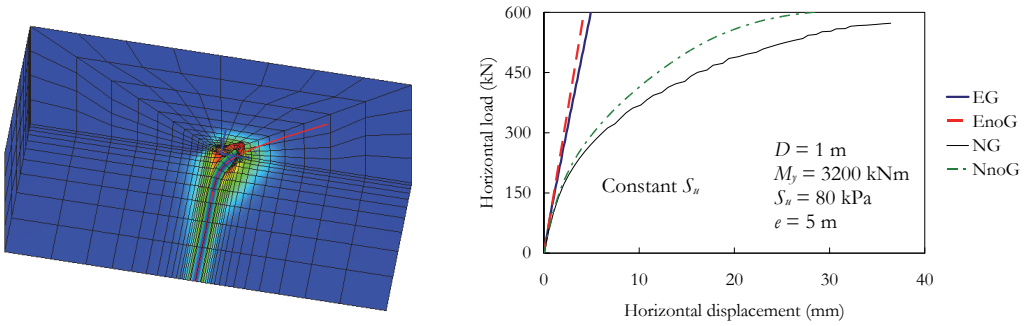

Figure 4. Gapping influence on the numerical response to pile-head loading for: elastic soil behaviour with and without gapping (EG and EnoG); full nonlinear response (NG and NnoG)

Based on these results, a nonlinear elastic constitutive model was proposed for elastic-gap behaviour. The gapping model assumed that the tangent flexibility matrix corresponds to an average between the initial elastic one, $\left(\mathbf{K}^{el}\right)^{-1}$, and the one with a full gap on both sides of the pile, $\left(\mathbf{K}^{gap}_{2\ sides}\right)^{-1}$:

$$\dot{\mathbf{Q}} = \mathbf{K}^{eg}\,\dot{\mathbf{q}}^{eg}, \qquad \left(\mathbf{K}^{eg}\right)^{-1} = \left(\mathbf{K}^{gap}_{1\ side}(z_{gap})\right)^{-1} = \left[\frac{1}{2}\left(\mathbf{K}^{el}\right)^{-1} + \frac{1}{2}\left(\mathbf{K}^{gap}_{2\ sides}(z_{gap})\right)^{-1}\right] \tag{2.1}$$

The current gap depth, z_{gap}, was assumed to depend on the relative distance from the current loading point and the failure surface, varying between zero and the soil wedge depth corresponding to the failure mechanism, z_w. Furthermore, a coupling with the plasticity model prevented this gap from closing completely, upon unloading, depending on the cumulative plastic displacement, u^{pl}_{cum}. The proposed evolution model for the current gap depth is then given by:

$$z_{gap} = \frac{z_w}{\lambda^{\beta}} \geq z^{\min}_{gap} = z^{\max}_{gap}\left(1 - e^{-\eta\, u^{pl}_{cum}/D}\right), \qquad z^{\max}_{gap} = \frac{z_w}{\left(\lambda_{\min}\right)^{\beta}} \tag{2.2}$$

where both β and η are calibration parameters and λ is a loading parameter (which decreases from infinity to one as the loading point approaches the failure surface). During unloading and reloading, and while the current gap depth is equal to $z^{\min}_{gap}$, Eqn. 2.1 is replaced by:

$$\left(\mathbf{K}^{eg}\right)^{-1} = \left[\frac{\lambda_{z^{\min}_{gap}}}{\lambda}\left(\mathbf{K}^{gap}_{1side}(z^{\min}_{gap})\right)^{-1} + \left(1 - \frac{\lambda_{z^{\min}_{gap}}}{\lambda}\right)\left(\mathbf{K}^{gap}_{2sides}(z^{\min}_{gap})\right)^{-1}\right], \qquad \lambda_{z^{\min}_{gap}} = \left(\frac{z_w}{z^{\min}_{gap}}\right)^{1/\beta} \tag{2.3}$$

2.3. Bounding Surface Plasticity Model

Bounding surface plasticity formulations assume that irrecoverable displacements develop before the yield/failure surface is reached. In fact, models based on this theory assume that the current plastic modulus, H^{pl}, continuously depends on the relative distance from the current loading point to its corresponding image point on the failure surface, as schematically shown in Fig. 5a.

The previously defined pile-head failure surface was assumed, in the proposed bounding surface plasticity model, to represent both a fixed bounding surface (i.e., with no hardening) and a plastic potential surface, thus corresponding to an associated plasticity model ($\mathbf{n}_f \equiv \mathbf{n}_g$). The elastic-gap-plastic tangent flexibility matrix may then be formally obtained by combining the additive decomposition of the displacement rate, the plastic flow and hardening rules and the consistency condition, similarly to classical plasticity formulations, resulting in:

$$\dot{\mathbf{q}}^{egp} = \dot{\mathbf{q}}^{eg} + \dot{\mathbf{q}}^{pl} = \left[\left(\mathbf{K}^{eg}\right)^{-1} + \mathbf{H}^{-1}\right]\dot{\mathbf{Q}}, \quad \mathbf{H}^{-1} = \frac{1}{H^{pl}}\left(\mathbf{n}_g \otimes \mathbf{n}_f\right) \tag{2.4}$$

A radial mapping rule was used, on the pile-head loading space, in order to define the image point: it projects the current loading point, from the origin, onto the bounding surface, as represented in Fig. 5b for the virgin loading state. The corresponding plastic modulus, H^{pl}, is determined by:

$$\delta = \frac{\Delta}{\Delta_{\max}} = \frac{1}{\lambda} \qquad \Rightarrow \qquad H^{pl} = H^{pl}_0 \ln\frac{1}{\delta} = H^{pl}_0 \ln\lambda \tag{2.5}$$

where H^{pl}_0 is a calibration parameter.

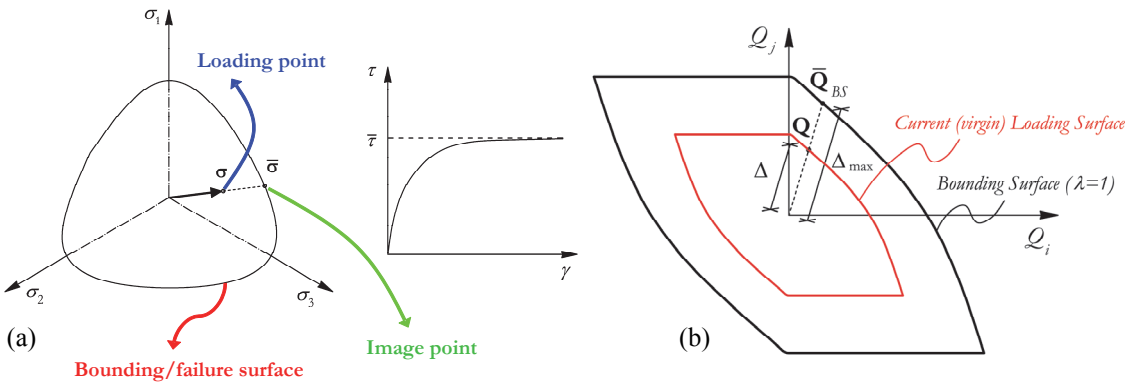

Figure 5. (a) Basic concept of bounding surface plasticity; (b) bounding and loading surfaces during virgin loading state

The behaviour during unloading and reloading states is determined through an analogous scheme, requiring another calibration parameter, n_{ur}. The proposed macro-element model thus calls for the following 15 input parameters to be defined: D, K_{HH}, K_{MM}, K_{HM}, $H_{u,\,e=0}$, M_y, n_H, n_M, γ, z_w, $(E_p\,I_p)_{eff}$, β, η, H_0^{pl} and n_{UR}. However, only the last four of these parameters have to be calibrated, since all the remaining ones are either known geometric and mechanic input data, or available in published literature, or given by the predictive relationships developed elsewhere. Further details may be found in Correia (2011). The pile-head macro-element was implemented in the seismic analysis software SeismoStruct (Seismosoft, 2011).

2.4. Macro-Element Validation

The advanced finite element results already shown in Fig. 4 were used for an initial validation of the macro-element response. It was calibrated and compared to such results both in terms of elastic and nonlinear responses, as well as monotonic and cyclic ones. Fig. 6 evidences the overall excellent agreement obtained after calibration for the results related to horizontal displacement. The adequacy of assuming associated plasticity behaviour is proven by the accurate results obtained also for the pile-head rotational behaviour.

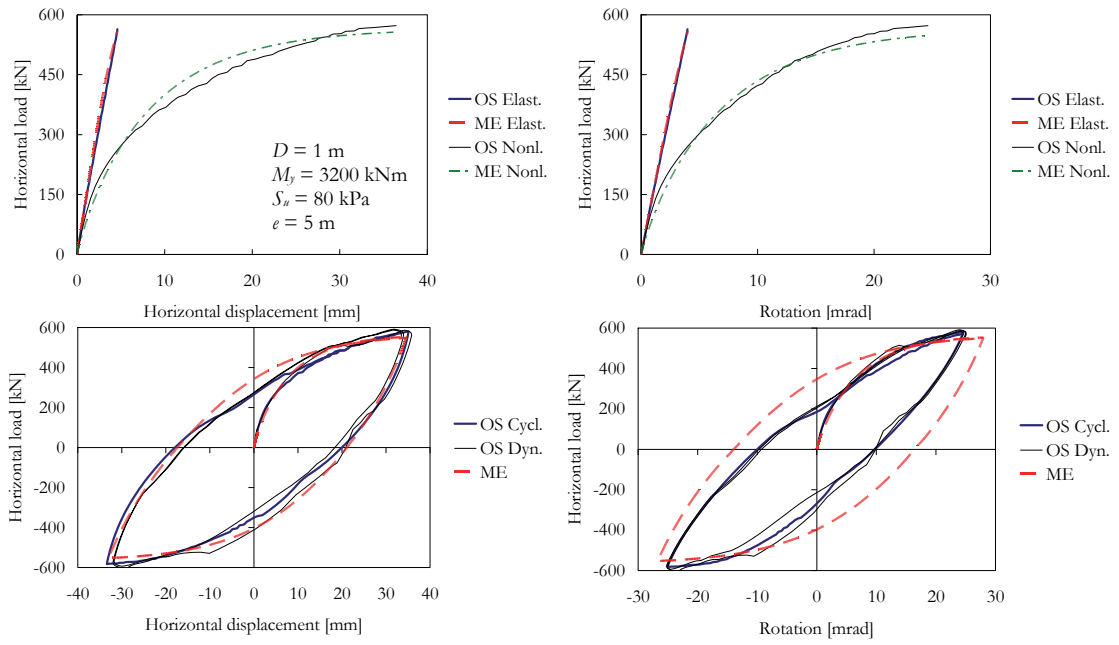

Figure 6. Macro-element (ME) vs. advanced finite element (OS) results for pile-head response

Further validation was accomplished by comparing the macro-element response obtained in a real lateral load free-head pile test (Stewart et al., 2007), to the corresponding macro-element results in terms of monotonic envelope and cyclic response. Fig. 7 represents such comparison, showing that the macro-element response is very close to the experimental one both in terms of maximum load attained for each cycle, unloading/reloading stiffness and overall hysteretic energy dissipation.

4. SEISMIC RESPONSE OF A MONOSHAFT-SUPPORTED BRIDGE

In this section, the reinforced concrete bridge structure, represented in Fig. 8, with pile/column supports and with regular geometry was studied. For evaluating the influence of SSI effects on its seismic response, three different support conditions were considered for the columns: fixed base, type II and type I monoshafts (also shown in Fig. 8). The latter two solutions correspond to alternative lateral design solutions for such supports: i) type I monoshafts, which adopt similar cross-sectional characteristics for both pile and column, will inevitably lead to an in-ground plastic hinge; ii) type II shafts, on the other hand, are capacity-designed so that the plastic hinge appears at the base of the column instead (SDC, 2010). Soil properties – which correspond to a soil type C medium/stiff clay saturated soil deposit according to EC8 – Part 1 (2003), deck dimensions and column/deck connection are also depicted in Fig. 8. Regarding the abutments, they are assumed to restrain torsional deck motions and to translate freely in the longitudinal direction, while having a bilinear response in the transverse direction. This ensures that the circular column design is optimised, corresponding to a similar behaviour in both directions.

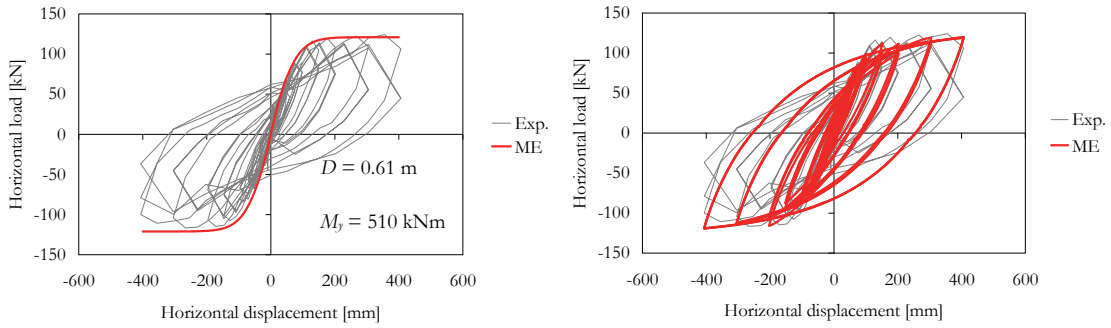

Figure 7. Macro-element vs. experimental results for pile-head deflection

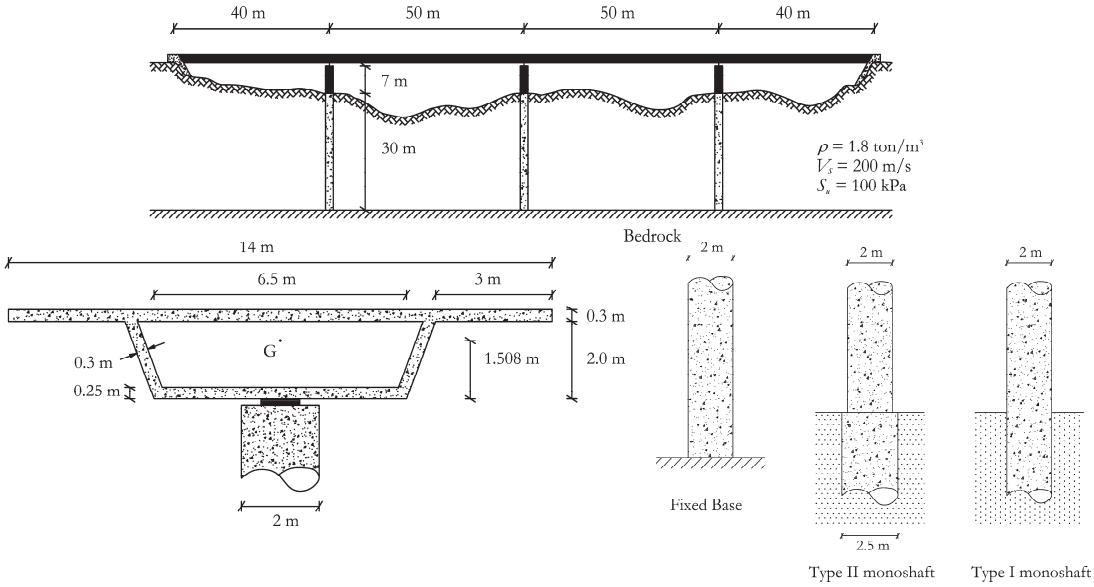

Figure 8. Bridge geometry, soil deposit characteristics and alternative design solutions

Additional modelling assumptions include: strain penetration effects in fixed-base columns were considered through equivalent elastic springs; an equivalent viscous damping of 2% was considered for the fixed-base case, which includes radiation damping effects; a smaller value of 0.5% was adopted for the other cases, since radiation damping was directly modelled in flexible-base solutions by using a couple of uncoupled eccentric equivalent dashpots connected to the pile-head (Correia, 2011).

Considering the fixed-base column, with a cross-sectional yield moment of 27 000 kNm, the yield lateral displacement was 45 mm. This value was roughly doubled for the type II monoshaft solution and tripled for the type I monoshaft support. It should be noted that second-order effects become significant for these columns when the lateral drift reaches values of the order of 0.5 to 1.0 m. While the first two solutions were allowed to reach a maximum displacement ductility demand of 4, the latter was limited to 3, since a plastic hinge forms below the ground surface for such solution (SDC, 2010). Regarding drift ratio code limits, the maximum value is usually limited to the interval 3-4.5%, while the residual value should not be larger than 1%.

The set of earthquake records used previously by Vamvatsikos and Fragiadakis (2010) was deemed appropriate for evaluating the seismic response of the bridge through nonlinear multi-record IDAs: 30 real ground motions selected for a small interval of relatively large earthquake moment magnitudes, 6.5 to 6.9, with moderate distances, 15 to 35 km, exhibiting no evidence of directivity and corresponding to a firm soil deposit for all time-histories. The cumulative absolute velocity (CAV) was chosen as intensity measure due to its predictability and adequate correlation to accumulated structural damage.

The behaviour of the macro-element model during the IDAs was very stable and cost-efficient, allowing for several thousands of analyses to be performed in a reasonable time frame. Fig. 9 exemplifies the column top and base displacements histories obtained, for a record acting in the longitudinal direction and scaled to CAV = 24 m/s. It is readily seen that second-order effects become significant for the type I monoshaft solution, leading to large residual deformations. Fig. 10, on the other hand, summarises the IDAs' results for the longitudinal direction in terms of the maximum column-top displacements, ductility demand (after removing the rigid-body motion due to pile deformation below the plastic hinge) and drift ratio. Finally, Fig. 11 depicts the residual column-top displacements and drift ratio. The residual values corresponding to the type I monoshaft solution are one order of magnitude higher than for the other solutions, as pointed out in Fig. 11. It is also noted that code-based limit values are explicitly represented in both Figs. 10 and 11.

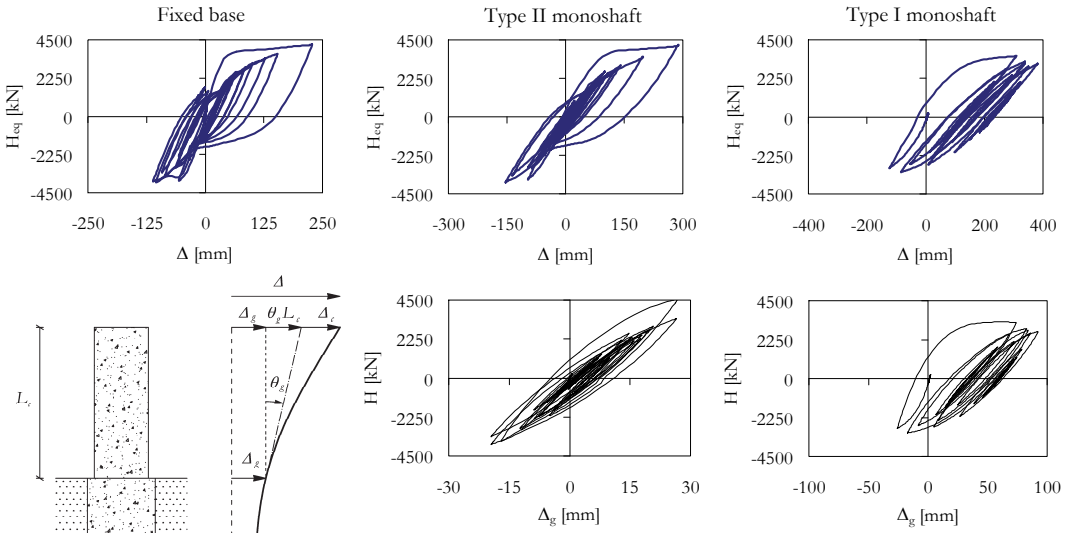

Figure 9. Example of load-displacement curves for tops and bases of the columns

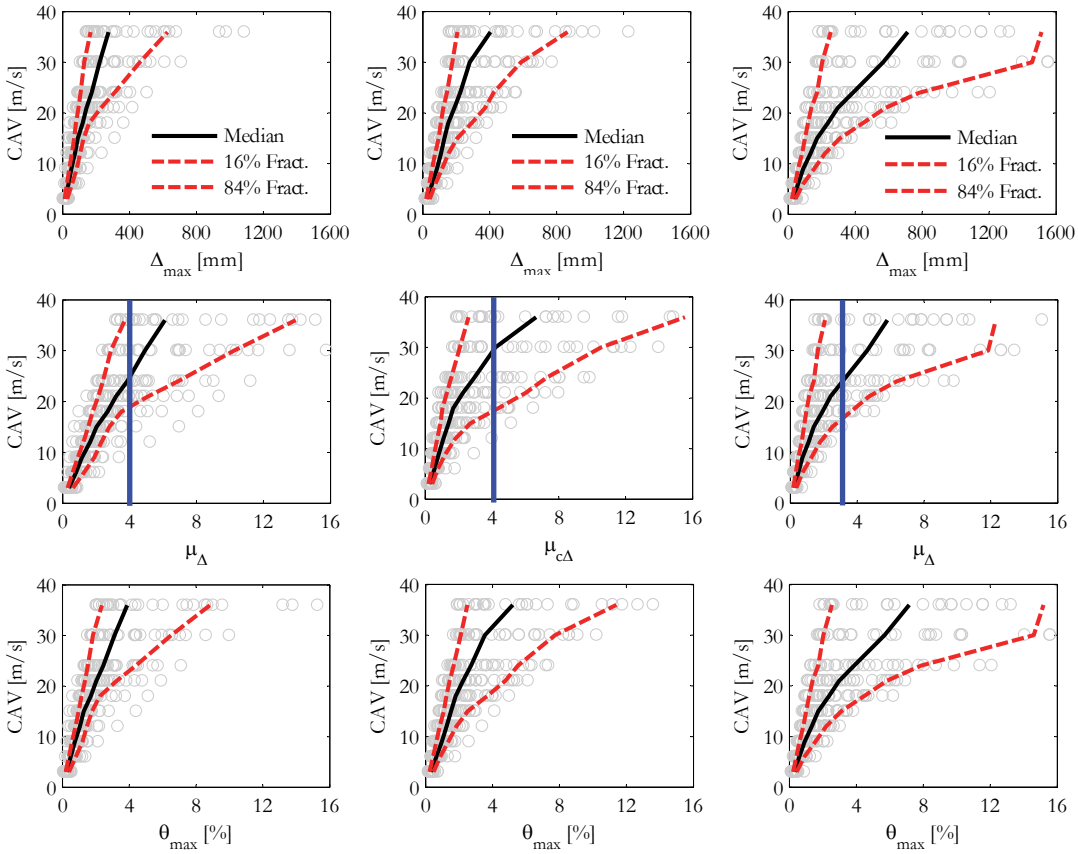

Figure 10. IDAs' maximum results: column-top displacement, ductility demand and drift ratio

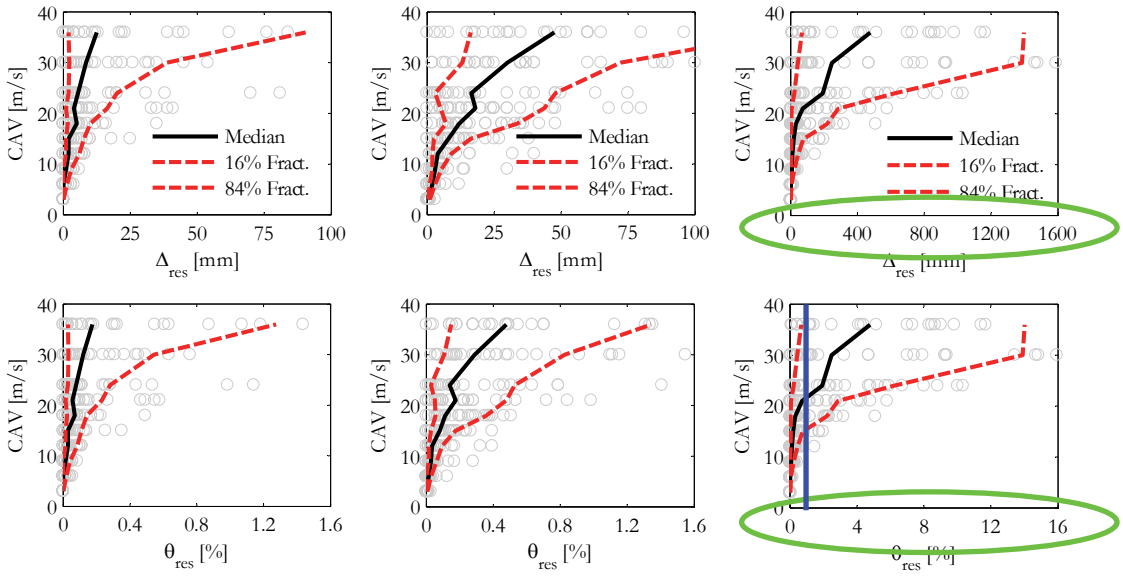

Figure 11. IDAs' residual results: column-top displacement and drift ratio

Obviously, flexible-base solutions show larger maximum displacements, which assume very significant values in the case of type I supports. The best performance in terms of code limits for ductility demand corresponds to the type II solution, whereas the other two structural solutions give similar values of maximum seismic intensity capacity. Nevertheless, type I supports lead to twice the drift ratio of the fixed-base solution, although they are also expected to have a larger plastic hinge length and rotational capacity due confinement provided by the soil at the plastic hinge location.

Regarding the residual values, these are negligible for the fixed-base case, more important but perfectly acceptable for type II supports and very significant for type I solutions at higher intensity levels. The performance of the latter is largely influenced by the significant second-order effects at high intensity levels for such a flexible structural solution. Additionally, the residual drift ratio limit of 1% in the type I solution is more restrictive, for this particular structure, than the ductility demand limit. For this case, such limit is respected by imposing a maximum design drift ratio limit of 3%, instead of the 8% value proposed by Song et al. (2006).

5. CONCLUSIONS

An innovative pile-head macro-element formulation was proposed and briefly described. Such formulation includes: a nonlinear elastic model, accounting for the transition from the initial response (with no gap), to a gap opening on the back of the pile (for monotonic response), or to a gap on both sides of the pile (when cyclic behaviour is considered – associated to the evolution of inelastic displacements of the pile-soil system); a bounding surface plasticity model ensuring a smooth evolution from initial nonlinear elastic behaviour up to full plastic flow at failure.

The proposed macro-element model was shown to adequately describe the main features of inertial SSI effects in the seismic response of pile/columns. Its response was successfully calibrated and validated for a set of existing results, both numerical and experimental. These validations confirmed that the macro-element is a valuable tool for accurate and efficient analysis of pile/column supports.

Afterwards, as an application example, nonlinear multi-record IDAs were performed on a reinforced concrete bridge with alternative support conditions. A statistical treatment of the results showed that, using the median values of the response, a smaller displacement ductility demand, after removing any rigid-body components, was attained with a more flexible solution. Considering that the damage at peak response in the supporting columns is proportional to the ductility demand, the damage potential was more pronounced for the fixed-base solution, decreasing for the type II monoshaft case and being least significant for the type I monoshaft solution. Nevertheless, the large flexibility of the latter induced significant second-order effects; consequently, significant residual displacements were produced. On the other hand, reasonable residual displacement values, and lower column damage than for the fixed-base solution, were obtained for the type II monoshaft solution. It is, therefore, considered to be the optimal structural solution for this simple example.

As a final conclusion, it should be pointed out that the extension of the macro-element concept to deep foundations was very successful. Moreover, the number of time-history analyses performed could hardly be accomplished without the stable response of such an efficient macro-element, which requires only a minor computational effort.

ACKNOWLEDGEMENTS

The first author wishes to gratefully acknowledge the financial support provided by the *Portuguese Science and Technology Foundation (FCT)* through the *Human Potential Operational Programme (POPH)*.

REFERENCES

Correia, A.A. (2011). A pile-head macro-element approach to seismic design of monoshaft-supported bridges, PhD Thesis, ROSE School, IUSS Pavia, Italy.

EC8 (2003). Eurocode 8: Design of structures for earthquake resistance, European Committee for Standardization (CEN), Belgium.

Figini, R., Paolucci, R. and Chatzigogos, C.T. (2011). A macro-element model for non-linear soil-shallow foundation-structure interaction under seismic loads: theoretical development and experimental validation on large scale tests. *Earthquake Engineering and Structural Dynamics*, **41:3**, 475-493.

Gazetas, G. (1991). Foundation vibrations. *Foundation Engineering Handbook*, 2nd ed., Fang, H.Y. (ed.), Van

Nostrand Reinhold, New York, USA, pp. 553-593.
Hutchinson, T.C., Boulanger, R.W., Chai, Y.H. and Idriss, I.M. (2002). Inelastic seismic response of extended pile shaft supported bridge structures. *Report PEER 2002/14*, Pacific Earthquake Engineering Research Center, University of California, Irvine, USA.
MathWorks (2009). MATLAB: The language of technical computing, Version R2009b, Natick, USA
McKenna, F., Fenves, G.L., Scott, M.H., Jeremic, B. (2000). OpenSees: open system for earthquake engineering simulation, version 2.1.0, available online from http://opensees.berkeley.edu, Pacific Earthquake Engineering Research Center, University of California, Berkeley, USA.
Pender, M.J. (2010). Earthquake Resistant Design of Foundations. *Course Notes*, ROSE School, IUSS Pavia, Italy.
Reese, L.C. (1958). Discussion of "Soil modulus for laterally loaded piles," by B. McClelland and J.A. Focht. *Transactions of the American Society of Civil Engineers* **123**, 1071-1074.
Salençon, J. (1983). Calcul à la Rupture et Analyse Limite, Presses de l'École Nationale des Ponts et Chaussées, Paris, France.
SDC (2010). Seismic Design Criteria – Version 1.6, California Department of Transportation (Caltrans), USA.
Seed, R.B., Dickenson, S.E., Riemer, M.F., Bray, J.D., Sitar, N., Mitchell, J.K., Idriss, I.M., Kayen, R.E., Kropp, A.L., Harder, L.F., Power, M.S. (1990). Preliminary report on the principal geotechnical aspects of the October 17, 1989 Loma Prieta earthquake. *Report UCB/EERC-90/05*, Earthquake Engineering Research Center, University of California, Berkeley, USA.
Seismosoft (2011). SeismoStruct 5.2.1: a computer program for static and dynamic nonlinear analysis of framed structures, available online from http://www.seismosoft.com, Pavia, Italy.
Song, S.T., Chai, Y.H. and Budek, A.M. (2006). Methodology for preliminary seismic design of extended pile-shafts for bridge structures. *Earthquake Engineering and Structural Dynamics* **35:14**, 1721-1738.
Stewart, J.P., Taciroglu, E., Wallace, J.W., Ahlberg, E.R., Lemnitzer, A., Rha, C., Khalili-Tehrani, P., Keowen, S., Nigbor, R.L. and Salamanca, A. (2007). Full scale cyclic large deflection testing of foundation support systems for highway bridges. Part I: Drilled shaft foundations. *Report UCLA SGEL-01*, University of California, Los Angeles, USA.
Vamvatsikos, D. and Fragiadakis, M. (2010). Incremental dynamic analysis for estimating seismic performance sensitivity and uncertainty. *Earthquake Engineering and Structural Dynamics* **39:2**, 141-163.